Journal of Coastal Research	29	6A	25–37	Coconut Creek, Florida	November 2013

Dynamics of Turbid Plumes Generated by Marine Aggregate Dredging: An Example of a Macrotidal Environment (the Bay of Seine, France)

Pierre-Arnaud Duclos[†‡§], Robert Lafite[†‡], Sophie Le Bot[†‡], Elie Rivoalen[††], and Antoine Cuvilliez[§]

[†]Université de Rouen, SFR SCALE
76821 Mont-Saint-Aignan Cedex, France
pa.duclos@gmail.com

[‡]CNRS, UMR 6143 M2C
76821 Mont-Saint-Aignan Cedex, France

[§]CNRS, UMR 6294 LOMC
76600 Le Havre, France

[††]INSA de Rouen
76801 Saint Etienne du Rouvray, France

www.cerf-jcr.org

www.JCRonline.org

ABSTRACT

Duclos, P.-A.; Lafite, R.; Le Bot, S.; Rivoalen, E., and Cuvilliez, A., 2013. Dynamics of turbid plumes generated by marine aggregate dredging: an example of a macrotidal environment (the Bay of Seine, France). *Journal of Coastal Research,* 29(6A), 25–37. Coconut Creek (Florida), ISSN 0749-0208.

On the French marine shelf, marine aggregates are currently dredged by trailing suction hopper dredgers (TSHD), without screening, with an overflow process, with or against currents. In the framework of the Groupement d'Interét Scientifique (GIS) Suivi des Impacts de l'Extraction de Granulats Marins (SIEGMA), the dynamics of the turbid plume formed by the overflow was studied at an experimental dredging site (0.6 km^2), located in the Bay of Seine (eastern English Channel), a macrotidal environment where the seabed is composed of sandy gravel. An original field strategy based on Lagrangian monitoring, using the back-scattered signal of an Acoustic Doppler Current Profiler (ADCP), Laser *In Situ* Scattering and Transmissometry (LISST) measurements, water samples, and aerial photographs, has shown good results in describing suspended sediment concentration (SSC) dynamics from a turbid plume. The behaviour of suspended sediment has been studied, for the first time, to our knowledge, from their release at the dredger overflow to their deposition on the seabed. A fluid mixture, overflowed from the TSHD, with a mean concentration of 6 g L^{-1} of mineral and organic silty sands, induces the formation of a turbid plume at the rear of the TSHD, with an immediate dilution effect about 10–100 on SSC. Then, the SSC decreases through the process of lateral dispersion and sedimentation until the plume disappear in 2 hours. Evolution of the plume characteristics (SSC, particle size and nature, geometry) makes it possible to quantify the processes involved: dilution, advection, dispersion, and settling. The passive and dynamic behaviours of the plume are analysed. Extensions of deposits are calculated for spring tide conditions: 800 m for sand and 6.5 km for silt. This study has been conducted in macrotidal and specific dredging conditions (orientation of the dredging tracks against currents, dredger speed, loading capacity, overflow type), whose effects on plume dispersion have been quantified. Indicators relative to the effect of the plume on the water column (I/R) and to the plume duration ($T_{1.25}$SSC) are proposed.

ADDITIONAL INDEX WORDS: *Aggregates, dredging, turbid plumes, environmental impact, sediments, eastern English Channel.*

INTRODUCTION

During the past few decades, marine aggregate extraction has increased in the English Channel (NW European marine continental shelf), which has submitted to other important anthropogenic pressures (*e.g.*, fisheries, maritime traffic, communication cables). Following the international recommendations (Rio de Janeiro, 1992, and Johannesburg, 2002), in an Integrated Coastal Zone Management context, it is necessary to achieve a better understanding of the physical impact of dredging activities on the seabed and the living resources.

The resuspension of particles generated by turbid plumes and their subsequent deposits induce several impacts on the environment: reduction of light penetration, increase of suspended solid particles and sedimentation rates, and changes in the superficial sediment type (Boyd and Rees, 2003; Cooper *et al.,* 2006; Desprez, 2000; Desprez, Pearce, and Le Bot, 2010; Le Bot *et al.,* 2010; Newell *et al.,* 2002; Robinson *et al.,* 2005). These physical effects can modify habitats and disturb the benthos (Boyd and Rees, 2003; Desprez, 2000; Desprez, Pearce, and Le Bot, 2010; Newell *et al.,* 2002, 2004) as well as benthic fishes (ICES, 2009; Stelzenmüller, Ellis, and Rogers, 2010). The dynamics of dredging plumes was studied from field surveys (Hitchcock, Newell, and Seiderer, 1999; Hitchcock, Newell, and Seiderer, 2002) and from models (Spearman *et al.,* 2007; Whiteside, Ooms, and Postma, 1995).

DOI: 10.2112/JCOASTRES-D-12-00148.1 received 29 July 2012; accepted in revision 18 January 2013; corrected proofs received 2 May 2013.

During dredging activities, two types of plume may appear: (1) a surface plume caused by the mixture of water and fine sediments released by overflow and screening processes, and (2) a benthic plume resulting from the disturbance of the seabed by the drag head or bucket of the dredger (Hitchcock and Drucker, 1996; Hitchcock, Newell, and Seiderer, 1999).

The present study investigates the dynamics of the turbid plume generated by aggregate dredging at an experimental dredging site, located in the Bay of Seine (eastern English Channel), a macrotidal environment in which the seabed is composed of sandy gravel. The dredging is operated by a trailing suction hopper dredger (TSHD), without screening, which is not allowed in France. The results focus on overflow mixtures discharged by shipside doors.

The sediment particles from the overflow are characterized based on their concentration, grain size, and grain type. An attempt was made to quantify the relative proportion of the different plumes (surface and benthic) from the concentrations of global resuspended matter. Plume source, shape, and dynamics were analysed according to the dredging operational conditions and hydrodynamic forcing. Finally the lifetime duration of the plume, as well as the area of its potential deposition, were evaluated in different hydrodynamic and dredging conditions. Thanks to an original and detailed field strategy and data processing, processes and controlling factors leading to the plume evolution were identified for the first time, to our knowledge. Indicators based on key parameters are proposed for (1) a better environmental risk assessment, (2) a comparison of these impacts for different dredging conditions, and (3) a comparison of these impacts on a larger scale (*e.g.*, eastern English Channel).

STUDY AREA

The area is an experimental site located in the eastern English Channel, on the continental shallow platform, between France and the United Kingdom (Figure 1a). The site is about 16 km offshore of Le Havre, France, to the west. It is situated in the Bay of Seine, in the extension of the Seine Estuary. The surface of the experimental dredging site measures 0.6 km^2, and the dredging activity is recent (<2 yr).

It is located at the extremity of the Seine bank (Figure 1b) and is Holocene in age (Auffret and d'Ozouville, 1986), which corresponds to the north alluvial terrace of the Seine (Auffret, 1982). The Holocene sediments are covered with a fine and mobile sandy-gravel (Folk, 1954) with 54% gravel, 44% sand, and 2% silt. This superficial layer can present weak lateral heterogeneities (Larsonneur, 1971). Cores sampled in early oceanographic surveys, taken by Alluvial Mining in 1972 and Centre National pour l'Exploitation des Océans (CNEXO) in 1976, showed a horizontal and vertical grain-size heterogeneity with the grain size increasing with depth. The water depth is between 20 and 23 m (lowest sea level measured in Le Havre). Tide and swell are the main forcing agents. Tides are semidiurnal, and the regime is macrotidal with a mean range around 7 m in spring conditions (SHOM, 2009). Tidal currents are dissymmetric in duration and intensity (Figure 1c and d). Flood and ebb currents can reach 1 m s^{-1} at the sea surface and decrease toward the sea bottom according to a logarithmic profile. The waves, a consequence of local winds, are less than 0.4 m high, more than 50% of the time lasting a short period between 4 and 6 seconds. Waves up to 1 m occur less than 10% of the time (data from Centre d'Études Techniques Maritimes et Fluviales).

Because of the proximity of the Seine Estuary, the study area is located in the transition zone between the open sea and estuarine waters (Gentil, 1976). Therefore, salinity and temperature present a small, vertical gradient and vary during the tidal cycles. The range of salinity is about 33–35. Temperature presents substantial seasonal variations, lowering to 6°C during winter and reaching more than 16°C at the beginning of autumn. The proximity of the Seine Estuary and biological activities induces variations in the suspended particle matter (SPM) concentration during the year and the tidal cycle (Avoine, 1987). This concentration can present a small, vertical gradient because of the biological and planktonic activities and the resuspension of fine sediments induced by strong currents and swell. Generally, the suspended sediment concentration (SSC) range is about 0.7–3 mg L^{-1} and can be more than 3.5 mg L^{-1} near the sea bottom. These data are in agreement with previous measurements (COB, 1978). The storm events increase the SSC by a factor of five in the whole water column (Dupont, Lafite, and Lamboy, 1985).

METHODS

Field Strategy

To describe natural parameters, such as tidal currents, salinity, temperature, and turbidity, 13-h time series were acquired in neap, mean, and spring tide conditions on the whole water column. The same parameters were also measured just before extraction for all monitoring surveys.

The study is based on *in situ* measurements of the plume characteristics from the dredger overflow to its dispersion in the water column and its deposition on the seabed. The adapted strategy is based on early recommendations for SSC study in the Bay of Seine (Lafite, Dupont, and Lamboy, 1985) and for dredging plume monitoring (Boutmin, 1986; Hitchcock, Newell, and Seiderer, 1999). Measurements were taken (1) on a monitoring vessel to measure the changes in the parameters in the water column and near the sea bottom, (2) on the TSHD to study overflow characteristics, and (3) from a helicopter to obtain a better overall view of the plume print near the sea surface. Two strategies were developed for monitoring. A Lagrangian strategy allows one to follow the turbid mass to measure the parameters in the same transversal cross-section of the plume throughout the plume's lifetime to evaluate sedimentation and dispersion of SPM. Measurements were repeated for different tidal conditions. Monitoring at a fixed distance from the dredger was also adopted, which measured possible change in plume characteristics during the loading sequence and any variation due to seabed heterogeneities. At the same time, on the dredger, samples were directly taken near the doors where overflow is rejected.

During the surveys, differential global positioning systems (DGPSs) with a 1- to 3-m accuracy were installed on the dredger and the monitoring vessel.

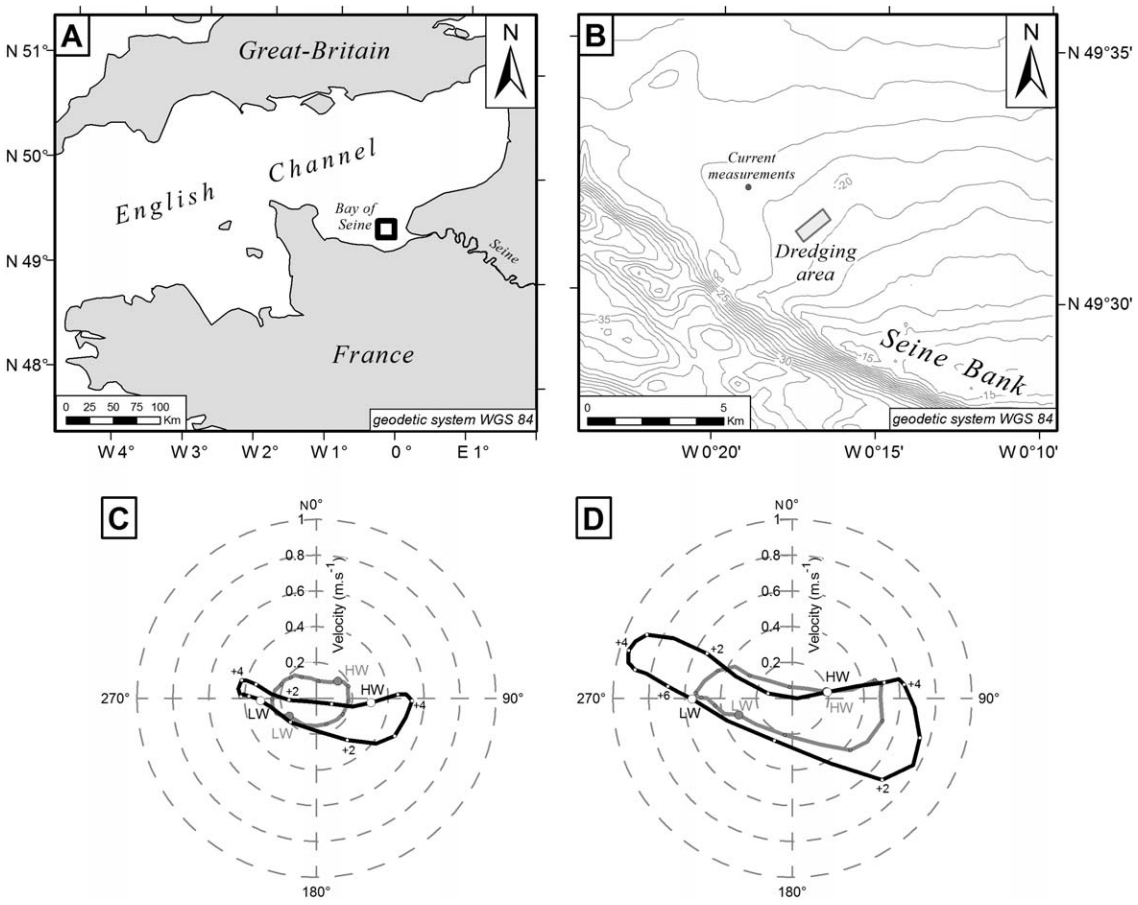

Figure 1. Location of the study area (A: English Channel and the Bay of Seine; B: Seine Bank and the dredging area, bathymetry data are from SHOM) and current diagrams (black: near surface ; grey: near bottom) during neap (C) and spring tide (D).

Parameters Studied, Instrumentation, and Data Processing

Current velocity and direction are measured with an acoustic Doppler profiler (ADP) connected to a pressure sensor and installed on a mooring system. Temporal and vertical hydrodynamic variations were studied during two neap–spring tidal cycles with a 1000 kHz ADP Sontek. The temperature and salinity were measured with a SBE 19 plus Seacat Profiler (CTD).

An ADCP Workhorse 600 kHz (RD Instruments) fixed on the monitoring vessel and oriented toward the seabed was used to study SSC. The ADCP echo intensity has been widely used to study natural SSC (Gartner, 2004; Tessier *et al.*, 2008) as well as to characterize dredging turbid plume (Hitchcock and Bell, 2004; Smith and Friedrichs, 2011). The ADCP echo intensity was calibrated in two steps. First, the echo intensity (I_{counts}) was converted into acoustic backscatter (I_{dB}) using Winriver 2 software (TRDI, 2007) using Equation (1) coupled with sound-absorption methods from Francois and Garrison (1982a,b):

$$I_{dB} = C \times I_{counts} + 20 \times \log_{10}\left(\frac{r + 0.5L_{X_{mit}}}{\cos\theta}\right) + 2\alpha R - 10 \times \log_{10}\left(\frac{L_{X_{mit}}}{\cos\theta}\right) \quad (1)$$

where r is the distance from the transducer to the middle of the bin, θ is the beam angle, $L_{X_{mit}}$ is the transmit length, α is the sound absorption coefficient, and C is the echo intensity scale. Then, the acoustic backscatter was calibrated using Equation (2), with SSCs measured from water samples collected at different depths (Figure 2):

$$\mathrm{SSC} = 0.0051e^{0.0813I_{dB}}, \qquad r^2 = 0.8187 \quad (2)$$

Particle grain size (Figure 3) was determined using a Sequoia type-C 100X Laser *In Situ* Scattering and Transmissometry (LISST) device. A similar instrument was used to characterize other dredging turbid plumes (Mikkelsen and Pejrup, 2000; Smith and Friedrichs, 2010). This instrument measures particles in the range of 2.5–500 μm. In the field, the LISST was deployed in the turbid plume on the same frame as the CTD probe, with all measurement cells at the same level

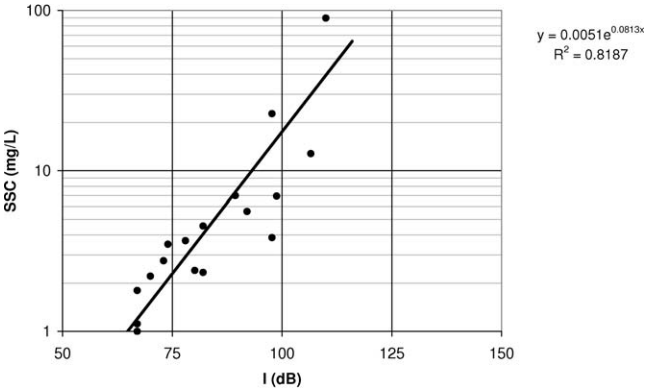

Figure 2. Calibration of the backscatter measured from ADCP.

above the seabed for a better correspondence between sedimentary and hydrodynamic parameters. In the laboratory on board, LISST was used to measure the grain size of the overflow sediment mixture sampled on the dredger. For the coarsest particles, water samples from the overflow were analysed in the laboratory with the particle-size analyser LS230 (Beckman) with a broader measurement range (0.04–2000 μm). To determine the particle type, samples filtered on polycarbonate membrane filters were observed on a scanning electron microscope (SEM) and analysed for x-rays. Filtrations were done immediately after sampling, allowing optimal floc conservation. Flocculation processes were observed during the dispersion of the plume, contrary to various previous studies (Mikkelsen and Pejrup, 2000; Smith and Friedrichs, 2011).

The disturbed ADCP (Hitchcock, Newell, and Seiderer, 1999) and LISST signals, induced by air bubbles from the overflow, the displacement of the TSHD, and the survey vessel, were removed. Therefore, ADCP and LISST data were acquired less than 10 minutes after overflow and near the surface (<4 m) were removed. There is also a thin layer of water near the bottom (10% of water depth) for which the ADCP data are poorly recorded.

RESULTS

In this macrotidal system, in calm conditions, with no extraction activity, the SSC range can reach 5 mg L^{-1}. Several time series have been acquired during tidal cycles. During flood phases and when wave activity occurs ($Hs > 2$ m), a vertical turbidity gradient was observed, with SSC values reaching 15 mg L^{-1} in the bottom part of the water column.

Source Characterization

The SSC of the overflow is essential data for understanding the evolution of the spill mixture coming out laterally from the eight shipside doors of the SandHarrier TSHD (CEMEX Marine), working without screening. During the loading time

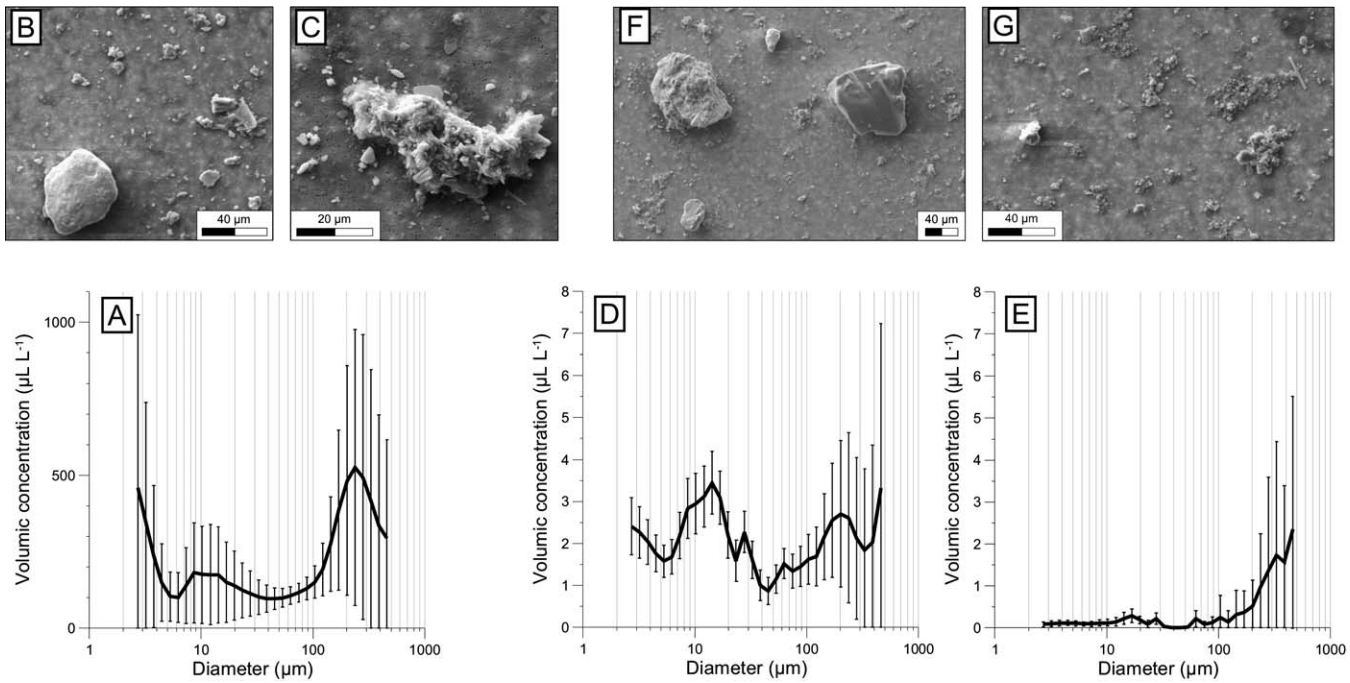

Figure 3. Characterization of the particles in the plume (A, D, and E: grain-size distributions of the particles in the overflow, the surface and the bottom plumes 10 min after the overflow start-up; B and C: SEM pictures of particles in the overflow; F and G: SEM picture of particles in the plume 10 min after the overflow).

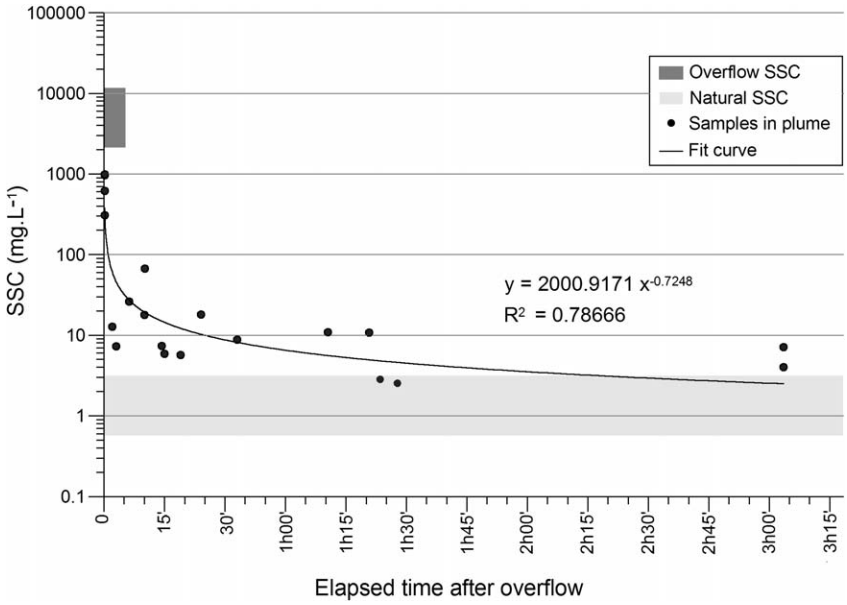

Figure 4. Suspended sediment concentrations in the surface plume. SSC ranges for the TSHD overflow (in dark grey) and the sea water (in light grey) including standard deviation.

on the study area—about 3 hours long—dredge-pump discharge was 4000 m^3 h^{-1} (N. Delsinne, CEMEX, *personal communication*), aggregate discharge into the hopper was approximately 850 m^3 h^{-1}, and the overflow discharge was around 3150 m^3 h^{-1}.

Water was sampled from the different spillway doors of the dredger: at the head and at the back, and both backboard and starboard. The SSC was about 6 g L^{-1} (range, 3–13) and was relatively constant during the loading period. The sediment composing the overflow mixture was a silty sand with 55.3% sand, 30% silt, and 14.7% clay. It was composed of four grain-size populations (Figures 3a–c). A small sand fraction around 700–800 μm was detected in water samples of overflow using the LS320. Other modes, detected by LISST, were in the fine to medium sand sizes (peak fraction, between 150 and 300 μm) and in the silt size (peak fraction, between 8 and 20 μm), comprising isolated mineral particles, bioclasts, mineral aggregates, and mixed organic–mineral flocs (Figures 3b and c). A last mode existed around 5 μm, represented by isolated mineral particles of a carbonaceous, siliceous, or clayey composition.

Subsurface Plume

The time evolution of the SSC in the subsurface plume was quantified from samples taken in the first water column layer (0–5 m deep) for various hydrodynamic and dredging conditions (Figure 4). The variability for SSC measurements corresponded to a normal statistical law. Theoretical ranges (significance level, 95%) of the SSC in the overflow and in the water column for natural conditions (*i.e.* without dredging activities) were obtained by adding and removing 2 SD to the average SSC values. Substantial dilution occurred when the overflow enters the water column at about 10–100 factor. Then, the SSC decreased as a logarithmic law (Figure 4). It decreased quickly in the first 10 minutes, from several hundred milligrams per litre to 20 mg L^{-1}. After 10 minutes, the SSC of the subsurface layer decreased slowly and tended to be similar to the background SSC after 2 hours.

The surface geometry and mobility of the plume were studied during a mean tide, during flood and ebb phases of a mean tide, as well as for slack waters (Figure 5a). The surface plume extension was mapped at the end of the loading using the surveys from the monitoring vessel and the pictures taken from a helicopter.

During slack conditions, a global plume extended up to 600 m around the dredging area. At other times, the plume propagated by advection in the direction of the tidal currents. During the ebb or flood periods, the overall plume extended as far as 6 km W and 8.5 km N–E, 100 m wide. The plume showed a quick lateral expansion during the first 0.5 hour after its creation, ranging from 50 to 100 m. On the aerial picture (Figure 5c), the plume boundaries are well defined for an overflow occurring less than 1 hour earlier. The upstream boundary of the plume is better defined and more linear than the downstream boundary, which is more diffused and presents some turbid vortices. For a 1-hour-old plume section, both boundaries are diffused. During the loading, TSHDs operated in the direction of the maximal length of the licensed dredging area (SW–NE) and turned in the opposite direction on the following track, approximately every 15–30 minutes. Because of the oblique direction angle between currents and dredging tracks, the different parts of the plume drew irregular chevrons. The direction, length, and width of the plume depended on the angle between the dredging tracks and the tidal currents. When the dredging

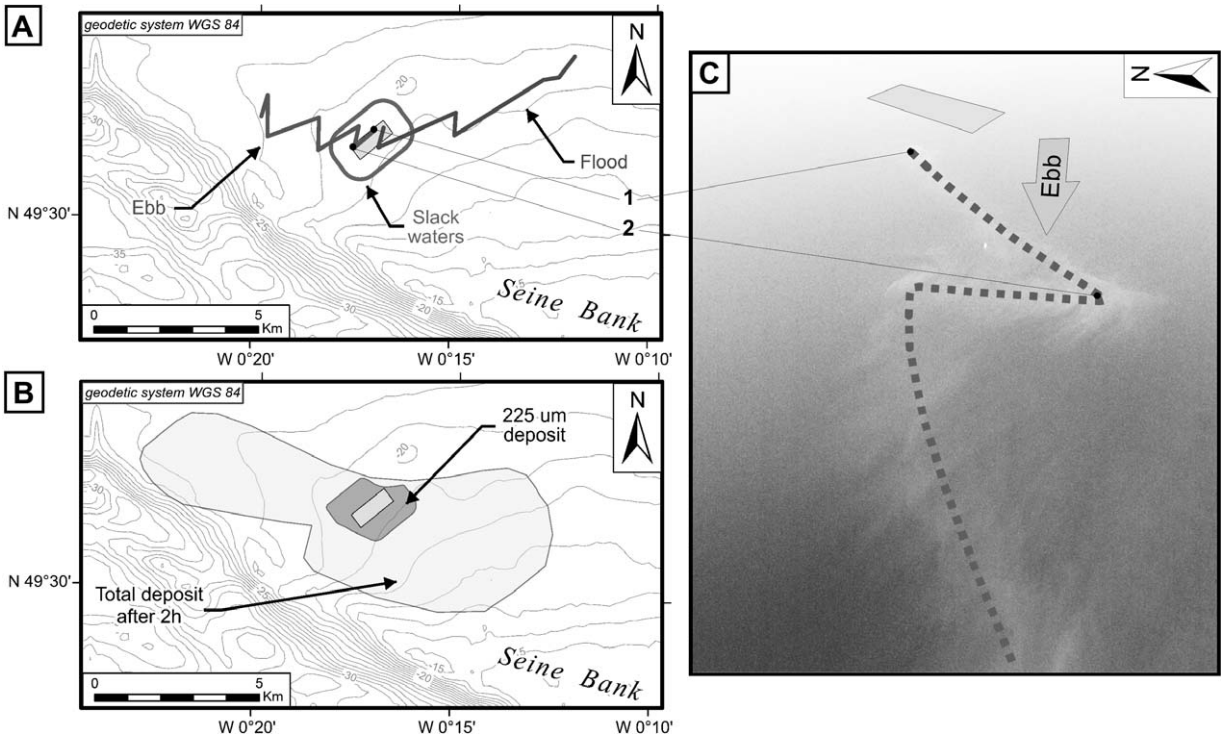

Figure 5. Sub-surface print of the plume and depositional area of sediment particles from the plume.A: sub-surface geometry for different tidal conditions during a mean tide B: Depositional area of sediment (light grey: maximum sediment deposition; dark grey: maximum extension for sand deposition area). C: Oblique picture taken from helicopter during ebb and neap tide.

track occurred in a direction having a larger countercurrent component, the plume part was longer than the with-current part was. Those parts were 3150 and 650 m long during floods, against and with currents, respectively, whereas the lengths were 1650 and 1250 m during the ebb tide. The width of the against-current part expanded to 200 m after 30 minutes; then, the plume extended slowly to exceed 300 m in width just before its visual surface disappeared, about 2 hours and 30 minutes after its creation. The width of the with-current part rose to 300 m more quickly (in 10 min); then, the width decreased, probably progressively. The dissymmetric chevrons were observed in neap, mean, and spring tide conditions (Figure 5a).

Plume Cross-Sections

Plume cross-sections (Figure 6) were acquired during a flood phase during neap tide conditions, with a plume formed against the currents. The boundary of the plume was defined to correspond to the background SSC plus two times the standard deviation. SSC spatial heterogeneities were observed.

Just behind the bubble trail at the back of the TSHD, 11 minutes after the overflow, the width of the plume's transversal section was about 100–150 m. The boundary shape was irregular and drew vortices between –10 and –15 m. The SSCs were heterogeneous and low in comparison with the high values in the overflow. The SSCs ranged between 1.4 and 21.6 mg L^{-1} from the boundary with background level at the centre of the plume. A cross-section showed that the plume was slightly more concentrated in the bottom part of the water column. After 15 minutes, the plume shape was simple, with vertical boundaries and a globally constant width from the sea surface to the bottom (Figure 6a).

Grain-size measurements (LISST data) indicated that the plume comprised the three finest modes that composed the overflow (Figure 3d and e). The nature of the particles was also similar. According to the SEM analysis, aggregates seemed to predominate (Figure 3f and g). However, vertical grain-size heterogeneities were observed in the plume. Near the sea surface, the plume was made of sandy silt with 40.2% sand, 49.8% silt, and 10.0% clay (Figure 3d), and the silt mode was predominant, instead of the overflow. Near the bottom, the plume was composed of silty sand with 82.5% sand, 15.2% silt, and 2.3% clay (Figure 3e). Sands were about seven times more predominant than the other modes, with particle sizes ranging from 201 to 460 μm. The finest mode was a very low-volume concentration, whereas the coarsest mode presented a concentration similar to that observed in the plume near the surface.

Cross-sections (Figure 6) show the plume's lateral dispersion up to 1 hour and 42 minutes. Between 15 and 36 minutes, two concentrated parts were clearly distinguished: one near the sea surface, and the other, larger, near the bottom (Figure 6a). From 36 minutes to 1 hour and 42 minutes, the SSC was higher in the centre of the plume, drawing a thin, less-concentrated vertical column (Figure 6b). Up to 1 hour and 42 minutes, near

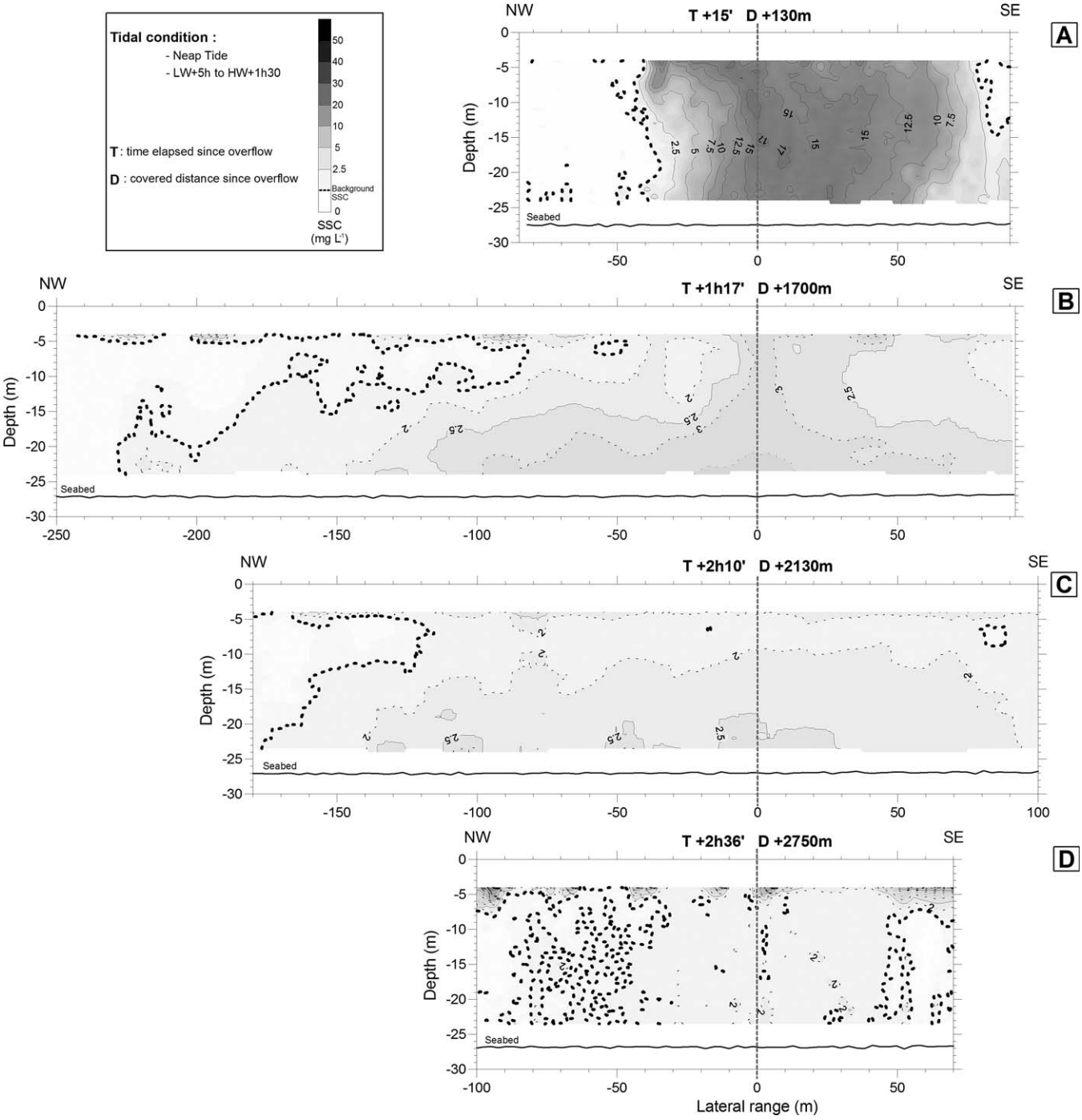

Figure 6. Cross-section evolution of the plume SSC 15′ to 2h20′ after the overflow. Cross-sections obtained in neap conditions, during a flood phase, from ADCP measurements by calibration of the echo intensity. The background SSC corresponds to the theoretical maximum SSC values in natural conditions, i.e. in absence of dredging activity.

the bottom, the plume extended laterally. After 2 hours, the column previously observed in the centre of the plume was no longer observed on the left. The more concentrated part, near the sea bottom, at that time poorly concentrated, was still observed 2 hours and 21 minutes after the overflow started (Figure 6c), but was no longer observed after 2 hours and 30 minutes (Figure 6d). Then, the lateral boundaries of the plume were difficult to localize, and the SSC tended toward the

background value. Note that the high values recorded near the sea surface seem to be induced by monitoring vessel turbulence (Figure 6d).

With plumes formed with the current, plume evolution was quite similar. The differences lay mainly in lower SSC values in the first part of plume lifetime and wider cross-sections.

Plume Longitudinal Time Evolution

The longitudinal time evolution from the overflow to the disappearance of the plume was studied by comparing each cross-section of the plume formed against the current, during the flood phase of a neap tide, in calm conditions (Figure 7). For every cross-section, SSC values were calculated for each water depth cell. They corresponded to a mean calculated from a vertical 5-m wide band centred on the most-concentrated surface value. Then mean values of every plume cross-sections were interpolated to produce the time longitudinal section (Figure 7b).

During the first half hour, the SSCs throughout the whole water column decreased to 11 mg L^{-1} and became homogenized, except at the sea surface, where SSCs were lower (Figure 7b and c). During the second half hour, SSCs continued to decrease progressively. During the second hour, the SSCs decrease was less, and the bottom SSC had a higher value. After 2 hours, the SSCs tended to reach the natural SSC progressively, with a small, positive, vertical gradient toward the bottom (Figure 7b and c). The surface of the plume cross-section (Figure 7d) increased until 1 hour and 42 minutes, with an irregular rate that comprised between 0.3 and 4.5 $km^2\ h^{-1}$ and decreased after 2 hours and 10 minutes with a mean rate around 6.4 $km^2\ h^{-1}$. This means that plume dispersion was observed for 1 hour and 42 minutes. The plume's lateral flux was calculated by comparing the variation in SSC from two successive cross-sections (Figure 7f). It corresponded to the ratio between the mean SSC surplus (Figure 7c) in the new plume surface and the time between those two cross-sections. Between 15 and 36 minutes, that rate was about 2.7 g s^{-1}. After that, it fell quickly and stayed low until 1 hour and 42 minutes. After 2 h, the horizontal dispersion was no longer observed (Figure 7f).

The sediment linear mass contained in the cross-sections decreased from 30 kg m^{-1} after 15 minutes to 0.4 kg m^{-1} after 2 hours 36 minutes (Figure 7e). The vertical flux decreases quickly, from 12.6 g s^{-1} to 2.0 g s^{-1} to 1 hour15 minutes (Figure 7f). After this, the rate stays globally constant, around 1.1 g s^{-1}. This evolution, observed throughout the plume's lifetime, demonstrates the settling of particles on the seabed. The comparison between the vertical and lateral rates (Figure 7f) shows that the settling is always 5 to 20 times greater than the lateral dispersion.

In the case of a plume formed with current, the plume time evolution presents SSC values that are twice as low in the whole water column, mainly during the first 45 minutes. Then the SSC decreased more slowly, inducing SSC values after 2 hours and 30 minutes close to the against-current values. A greater transversal extent associated with lower a SSC causes a greater mass *per* linear meter value up to 1 hour15 minutes.

The volume concentrations obtained from the LISST are close to the background values 1 hour15 minutes after the overflow (Figure 7a). At that time, all coarse particles have settled on the seabed except near the surface where coarse biological particles and aggregates are probably still maintained with two modes: the first one between 63 and 170 μm and a second one coarser than 330 μm. At the beginning (10 minutes), the plume is mainly made up of the finest particles (<63 μm) with a concentration maxima between 10 and 15 m in depth. The plume is made up of silty sand or sandy silt from the surface to 7.5 m deep and to silt between 7.5 and 20 m. Then the deeper measurement between a depth of 20 and 22.5 m shows silty sand. Near the bottom, the two finest modes and a third mode around 200 μm similar to the coarse particles observed several minutes after the overflow are in equal proportions. The mode composed of very fine silt and mud and the silt mode are still present in the same proportion throughout the water column. Flocculation seems not to have been active during plume evolution.

Deposit

Recent side-scan sonar and sediment data did not show evidence of overflow deposits. Two reasons can be put forward: (1) insufficient amounts of overflow because the dredging has begun recently (about 2 years before measurements) and is operated with a weak intensity (about 2 h and 30 min *per* year *per* hectare), and (2) the high mobility of deposits quickly reworked by currents and waves after their deposition.

The maximum deposit extensions of particles from the plume can be evaluated. As shown before, we can consider that the plume has settled after 2 hours. The maximum distance where particles can be deposited is estimated from the residual water movement induced by currents occurring over 2 hours (the semi-diurnal tidal cycle used has a 30-min time resolution).

During spring tides, the finest particles (<63 μm) contained in the plume can settle up to 6.5 km around the dredging area for an overflow appearing during a flood phase, 3–4 hours after low water (Figure 5b). The extension of the maximum deposit of the fine sands is estimated according to the Zanke equation (1977). As measured by the LISST, the overflow partly comprises organic mineral fine sands (including aggregates), which mainly settle in 1 hour09 minutes (Figure 7a). A settling velocity of 0.028 m s^{-1} has been calculated for sand (mineral particles) measuring about 225 μm based on Zanke equation (3):

$$W_S = \frac{10\upsilon}{D}\left[\left(1+\frac{0.01(s-1)gD^3}{\upsilon^2}\right)^{-1}-1\right] \qquad (3)$$

with υ the kinematic viscosity in Pa s^{-1}, D the particle diameter in m, s the relative density of particle with respect to water density and g the gravity coefficient in N kg^{-1}. For spring conditions, the time to deposit mineral sand on the seabed ranges from 12 to 17 minutes, depending on the moment considered in the tidal cycle and the subsequent evolution of the water level. Then the deposition distance has been calculated using the residual current velocities and their direction occurring at different moments along the tidal cycle. A maximum distance of 800 m is estimated for the deposition of

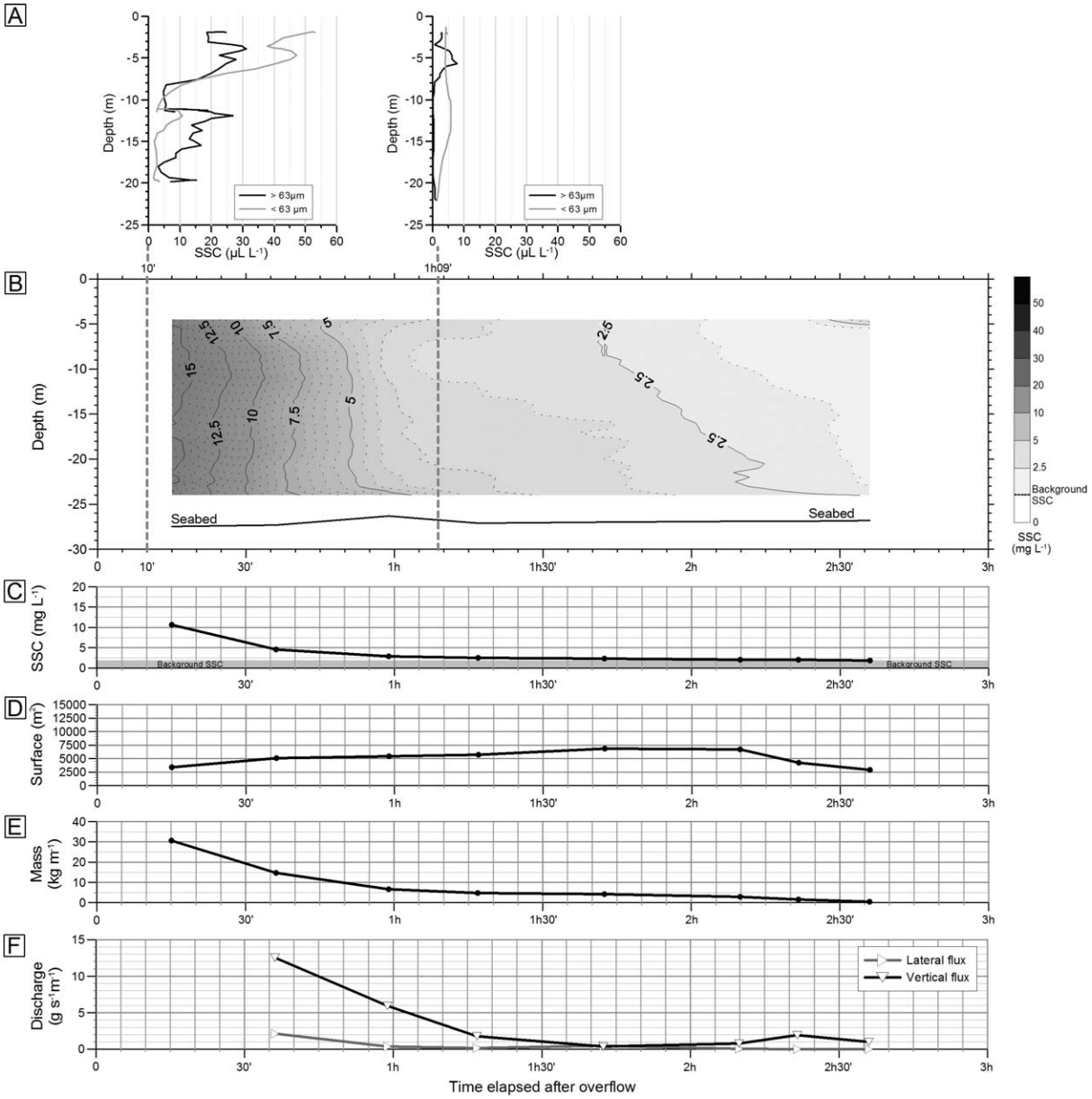

Figure 7. Time evolution of plume formed against currents during the flood phase of a neap tide, in fair weather conditions (A: vertical grain-size profiles 10′ and 1h10′ after overflow; B: SSC along the water column as a function of time in the center part of cross-sections; C: mean estimated SSC evolution; D: surface of cross-section; E: total mass of particles in the cross-section; F: lateral and vertical fluxes).

the fine sand mode around 225 µm in case of an overflow occurring during a flood phase, 3–4 hours after low water (Figure 5b).

DISCUSSION

The dynamics of the turbid plume generated by aggregate dredging is studied at an experimental dredging site in the Bay of Seine (Eastern English Channel). This required determining the water column characteristics in normal conditions and with dredging activities. In the macrotidal conditions of the Bay of Seine, currents reach maximum velocities of 1 m s^{-1} at the sea surface (Figure 1), which induce shear stress velocities reaching 0.04 m s^{-1} on the seabed during calm periods and 0.09 m s^{-1} during storm periods. Resuspension is observed during flood periods and during periods of wave activity, displaying a vertical gradient.

Plume Dynamics

Plume dynamics in case of dredging can be summarized and its processes can be specified (Figure 8).

Plume Origin

During dredging activities, two types of plumes may appear: a surface plume due to the mixture of the water and fine sediments releases by overflow and a benthic plume due to the disturbance of the seabed by the drag head of the TSHD or bucket of the static dredger (Hitchcock and Drucker, 1996; Hitchcock, Newell, and Seiderer, 1999). The main cause of turbidity is the release of excess water at the sea surface by the dredger overflow (Hitchcock, Newell, and Seiderer, 1999). The plume, formed at the rear of the TSHD, a short time after the overflow dilution (10 min), comprises two high-concentration zones: (1) one near the surface with a SSC above 15 mg L^{-1}, with a majority of silts coming from the surface plume, and (2) another one close to the bottom (around 20 mg L^{-1}) due to the settling of coarse particles. The contribution of a benthic plume generated by sediment suspension during the passage of the drag head was measured by Hitchcock, Newell, and Seiderer (1999) with a low concentration (31–37 mg L^{-1}) and a small transversal surface. In the present study, this effect is not observed or measured due to the lack of measurements before 11 minutes and a blind zone 4 m thick above the bottom.

Plume Behaviour

Beyond 11 minutes, two slightly more-concentrated areas (several milligrams *per* litre) were observed, one drawing a narrow vertical column visible up to 1 hour and 42 minutes and a wide 12.5-m-thick area observed above the bottom up to 2 hours and 21 minutes. These geometries were similar to those observed in open water disposal activities (Truitt, 1988) during the dynamic phase and the associated density current, which was spread over the bottom. For plumes associated with aggregate dredging, Dankers (2002) distinguished (1) a dynamic behaviour, defined by a fall velocity of all particles greater than one of the single particles, associated with a density current on the sea bottom; and (2) a passive behaviour that displays a fall velocity of all particles smaller than one of the single particles. Previous research also suggests the existence of a quick dynamic phase in the case of aggregate dredging in a fixed point with no screening (Hitchcock and Bell, 2004), in a time interval of 5–10 minutes for the overflow from a well (Whiteside, Ooms, and Postma, 1995) and within the first 10–15 minutes in the case of an overflow from a well with screening (Hitchcock, Newell, and Seiderer, 1999). Spreading on the bottom of part of the suspensions in the form of a density current, called the *near-bed plume*, has been described (Hitchcock, Newell, and Seiderer, 1999; Hitchcock and Bell, 2004; Spearman *et al.,* 2007; Whiteside, Ooms, and Postma, 1995). This near-bed plume extends up to 800 m in the direction of the currents and is 3–4 m thick when overflow comes from a well (Hitchcock, Newell, and Seiderer, 2002) and can extend up to 8 km in aggregate dredging with screening (Dicksons and Rees, 1998 in Newell *et al.,* 2004).

In our study, based on ADCP measurements, a significant anomaly of down vertical velocities from 0.01 to 0.04 m s^{-1} was observed in the plume up to 12.5 m above the sea bottom (for cross-sections measured 11 min and 15 min after the overflow). These speeds were induced by the settling of the SPM but were smaller than the fall velocity of individual particles that made up the lower part of the plume at that time (201–460 μm). A dynamic phase occurring after 11 minutes, therefore, did not exist. The most-concentrated areas of the plume, which drew a narrow, vertical column and spread on the sea bottom, were not associated with a dynamic phase or a density current.

During the first 10 minutes after overflow, the vertical velocity field measured by the ADCP was not workable because of the bubble wake induced by the TSHD and the overflow. The classification diagram of Winterwerp (2002), concerning the behaviour of surface plumes, indicated that the plumes occurring in our study conditions should have had a mixing behaviour associated with the mean values of the Richardson number *Ri* and the velocity ratio ζ. Therefore, the plumes may not have been affected by a dynamic phase but only by a passive phase, except for the extreme values of both parameters (the increase of overflow concentrations and the decrease of current velocity relative to the dredger). Apart from those extreme conditions, the most-concentrated area of the plume, which drew a narrow, vertical column, may have been closely associated with the fall of denser and/or larger particles that were less sensitive to the lateral dispersion that would separate it from the rest of the plume by settling faster on the bottom. The most-concentrated area observed on the sea bottom may be associated with a permanent suspension phenomenon of the finest particles because of the turbulence on the sea bottom, the resuspension of previous plume deposits, and/or the contribution of benthic plume particles induced by the drag head passage. In conclusion, the passive phase that characterized the dynamics of this overflow plume was subjected to settling and lateral dispersion.

Plume Deposit

The plume deposits of this recent extraction (<2 years) have not yet been observed on side-scan sonar. From calculations, it can be assumed that fine sands can settle within 800 m around the extraction area, and deposition of the finest particles can extend up to 6.5 km (Figure 5b).

Boutmin (1986) calculated a maximal distance for water mass movement and sediment deposit about 4 km off the Loire estuary. In the Baltic, Gajewski and Uscinowicz (1993) observed deposits up to 1 km in the direction of the current, extending about 100 m on both sides of the dredger track. In a dredging area, located off Dieppe (France), in the English Channel, overflow deposits (fine sands) may extend beyond 2 km away from the downstream boundary of the dredging site because of a reworking of the fine sands after their deposition by tidal currents (Desprez, Pearce, and Le Bot, 2010; Le Bot *et al.,* 2010). A similar distance was detected in an aggregate extraction site in the southern North Sea (Robinson *et al.,* 2005) under similar current conditions (rectilinear tidal ellipse, maximum spring tidal current velocity reaching 1.5 m s^{-1}).

The nature and extent of these deposits are influenced by the size and nature of the dredged material and the tidal currents. It is evident that the presence of deposits depends on dredging characteristics (total mass rejected by overflow and dredging intensity) and reworking (erosional critical velocity). A field survey focused on sand deposits around a

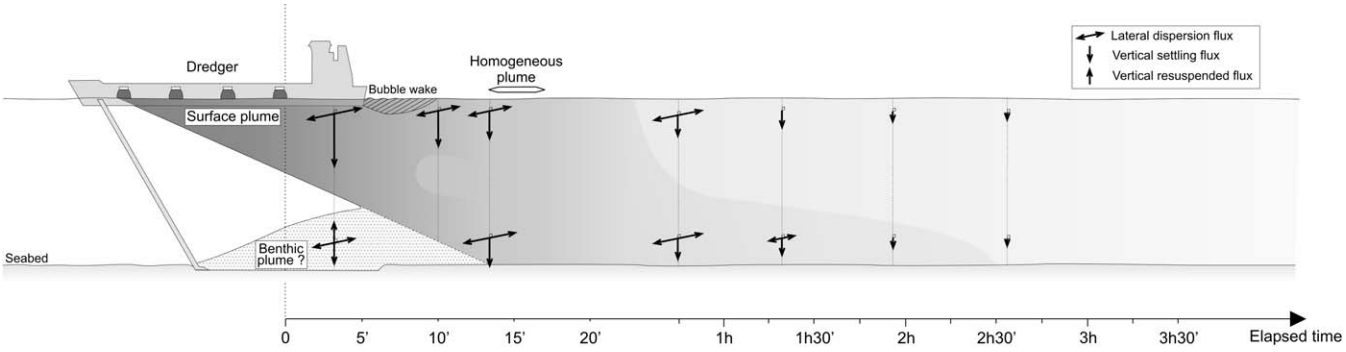

Figure 8. Conceptual model for the dynamics of a dredging plume in a macrotidal environment.

dredging area off Dieppe (Le Bot *et al.,* 2010) with similar hydrodynamic and sedimentary characteristics has shown an extension farther than the theoretical extent calculated here. We can assume that this farther extension was due to reworking by swell and tidal currents. In the dredging area in the Bay of Seine, the absence of deposits on side-scan sonar could result from the characteristics of the extraction (recent) and/or by reworking.

Influence of Dredging Practices

Indicators based on key parameters are necessary to easily and rapidly qualify and quantify environmental impacts to be able to compare the effects of different dredging practices and environmental conditions. These tools can be used to help define the best practices to limit the physical and biological effects of dredging plumes on the environment.

Current Direction and Velocities vs. Dredging Tracks

From our results, a $T_{1.25}$SSC indicator was proposed that corresponds to the time elapsed between the overflow start-up and the moment when the plume SSC represents not more than 1.25 times the natural SSC. This indicator can describe plume disappearance and compare plume dispersion time according to the dredging (relative current from the dredger, spill type, pump discharge, and hopper capacity) and environmental conditions.

The geometry (boundaries, length, and width), SSC, and dynamics of the plume depend on the direction and velocities of the currents compared with the dredging tracks. In our case, $T_{1.25}$SSC was 2 hours and 13 minutes for dredging against the current and 2 hours and 8 minutes for dredging with the current. This indicator could be calculated for other dredging areas from data obtained during previous studies. For dredging areas off the British coast in the eastern English Channel, the $T_{1.25}$SSC for the plume formed without screening is 0 hours and 56 minutes on Owers Bank (Hitchcock, Newell, and Seiderer, 1999) and 0 hours and 39 minutes off Eastbourne (HR Wallingford, 2011).

During with-current conditions, a greater SSC inducing a longer disappearance time was expected, contrary to the field observation. The faster speed of the dredger during the with-current track could induce lower SSC in the overflow, which might explain this difference.

The shortest length of the subsurface plume was obtained with extraction carried out with the current; that indicates that plume sediments will deposit on the seabed within a smaller area than for an extraction made against the current.

Nevertheless, the relative angle between dredging tracks and currents (with- or against-current dredging conditions) seems to be a major factor controlling the initial plume concentration, plume geometry, and plume dynamics (mainly dispersal component), but not the plume disappearance time and the extension beyond the dredging area, both of which were independent of dredging conditions.

Dredger Characteristics

This study examined dredging activities for a spill-type rejection (ship-side doors) with medium pump discharge and overflow discharge, compared with those of the other dredgers working in the world. Further combinations of scenarios may be considered according to the type of dredging (anchor or trailer dredging), the loading capacity of the dredger, the pump discharge, the kind of overspill (central column or ship-side spillway), and the presence or absence of screening. These different scenarios will change spill discharge, the rejected SSC, and the total weight of rejected particles.

Indeed, other TSHDs are used in the study area, such as the Charlemagne (DEME). This dredger has a larger hopper, a greater aspiration discharge, and an overspill through a central spillway. Measurements have shown an overspilled SSC of around 19 g L^{-1} (range, 5–31) for the Charlemagne, greater than the 6 g L^{-1} (range, 3–13) SSC of the SandHarrier. With that SSC and its overspill characteristics (higher overflow velocities), the overflow discharge would be higher: about 145 t h^{-1} for the Charlemagne, compared with 19 t h^{-1} for the SandHarrier. That substantial difference in spilled-sediment discharge must be balanced with the greater extraction yield obtained by the Charlemagne. Indeed, the Charlemagne hopper, twice as large as the SandHarrier hopper, fills in a shorter time, implying a shorter pressure time on the seabed. The I/R indicator quantifies the extraction efficiency. It corresponds to the ratio of the volume of suspended material

released by overflow from the dredger to the loaded volume in the hopper. This value has already been proposed by Hitchcock, Newell, and Seiderer (1999). The I/R indicator is three times higher for the Charlemagne (0.046) compared with the SandHarrier, despite a higher loading discharge for the Charlemagne.

The dynamic phase is possibly observed when the Charlemagne's overflow characteristics are considered. The Charlemagne's overflow characteristics have been implemented in the Winterwerp's diagram (2002) and clearly show that the plume has a different behaviour compared with that of the SandHarrier's plume.

When screening is allowed, it will radically change the behaviour of the plume (Hitchcock, Newell, and Seiderer, 1999, 2002) by increasing the SSC value, the particle grain-size and the loading time. Therefore, the total weight of sediment rejected will be clearly higher and the plume dynamics will include a dynamic phase.

CONCLUSION

This study covered a small area (0.6 km^2) submitted to recent, experimental dredging activity (<2 y). It is located in a macrotidal environment (eastern English Channel), where the seabed is about 20–23 m deep and is composed of gravel and sand.

The dynamics of turbid plumes generated during the extraction of marine aggregates can be studied by analysing the characteristics of the overflow (SSC, particle grain size, and nature) and using hydrosedimentary Lagrangian monitoring of the plume (ADCP and LISST). However, the presence of a trail of bubbles at the rear of the dredger, during the first 10 minutes after the overflow, makes it impossible to analyse the dynamics of the plume in that time interval.

The plume formed at the rear of the dredger is mainly due to the release of particles from the dredger by overflow. The overflow from ship-side doors is composed of silty sands with a 6 g L^{-1} SSC. When it enters the marine environment, the overflow SSC decreases abruptly by dilution by a factor of 10 to 100. In the plume, the SSC will decrease according to a logarithmic law, rapidly in the first 10 minutes (20 mg L^{-1}) and then gradually (10 and 5 mg L^{-1} after 30 min and 1 h, respectively). The sands will drop quickly within the first 12–17 minutes and, beyond, the plume will consist primarily of silts.

In the case of an overflow from ship-side doors, the plume behaviour is passive, whereas the evolution of cross-sections may show geometries typically observed in a dynamic phase. In the case of an overflow *per* well, the plume may also display a dynamic phase. During the passive phase, the SSC decreases through the process of lateral dispersion and sedimentation (Figure 8). The proportion of these different phases (dynamic or passive) depends on the overflow (central well or ports), whether or not screening is carried out, and the current velocity relative to the dredger.

In this macrotidal context, the extraction conditions (dredging with or against current, suction pump discharge, loading capacity, overflow type, whether or not screening is carried out) control the initial SSC, the plume geometry (in this study by irregular "chevrons"), and its dynamics, but not its dispersion time and its extension beyond the dredging area.

The dredged material (grain size and type) and tidal currents determine the plume mobility and the extension of the associated plume deposits. The finest deposits can be observed up to 6.5 km beyond the dredging area during the flood phase, and the fine sands can be observed up to 0.8 km. The size of these deposits will depend on dredging characteristics, such as the total mass rejected by overflow, the dredging intensity, and the erosion-critical velocity controlling the reworking of sediment after its deposition.

Indicators, based on SSC as well as the loaded and released sediment volumes, are provided to easily and rapidly quantify their environmental impacts to be able to compare the effects for different dredging and environmental conditions. Consistent with the objectives of the GIS SIEGMA, management tools should be proposed for all physical (water column and bottom) and biological (benthos and fish) compartments.

ACKNOWLEDGMENTS

This work was funded by Les Graves de l'Estuaire and the ANRT under CIFRE no. 708/2007, and by the "GIE GMN" as part of the GIS SIEGMA scientific programme of the supported by the Research Federation SCALE 4116. The authors extend their thanks to the crews of the RV *Côte d'Aquitaine*, the *Côtes de la Manche* (INSU/CNRS), and the *Thalia* (Genavir/Ifremer) who made the field data collection possible. Also, the assistance of Nicolas Delsinne, Carole Brunaud, Yann Ferret, Olivier Blanpain, Michel Desprez, Julie Gonand, and Michel Simon during the surveys or in the laboratory is highly appreciated. The Hydrographic and Oceanographic Office of the French Navy (SHOM) is acknowledged for providing bathymetric data.

LITERATURE CITED

Auffret, J.P., 1982. *La Manche: Paléovallées et bancs sableux*. Orleans and Issy-les-Moulineaux, France: BRGM–Ifremer, scale 1 : 500,000.

Auffret, J.P. and d'Ozouville, L., 1986. *Cartographie du prisme sédimentaire holocène en baie de Seine orientale, par sismique réflexion a haute définition*. La Baie de Seine (Greco Manche)—Colloque National du CNRS. Plouzané, France: Ifremer, pp. 201–210.

Avoine, J., 1987. Sediment exchanges between the Seine estuary and its adjacent shelf. *Journal of the Geological Society of London,* 143(1–14), 1301–1305.

Boutmin, G., 1986. *Dragage et Exploitation des Sables Marins: Qualité des Matériaux et Conséquences sur le Milieu*. Nantes, France: University of Nantes, Ph.D thesis. 187 pp.

Boyd, S.E. and Rees, H.L., 2003. An examination of the spatial scale of impact on the marine benthos arising from marine aggregate extraction in the central English Channel. *Estuarine, Coastal and Shelf Science,* 57(1–2), 1–16.

COB (Centre Oceanologique de Bretagne), 1978. *Baie de Seine, Campagne Thalia mai 1978, Présentation des Résultats*. Brest, France: CNEXO-COB, 189p.

Cooper, K.M.; Boyd, S.E.; Aldridge, J., and Rees, H., 2006. Cumulative impacts of aggregate extraction on seabed macroinvertebrate communities in an area off the east coast of the United Kingdom. *Journal of Sea Research,* 57, 228–302.

Dankers, P.J.T., 2002. *The behaviour of Fines Released Due to Dredging: A Literature Review*. Delft, Netherlands: Hydraulic

Engineering Section, Faculty of Civil Engineering and Geosciences, Delft University of Technology. 59p.
Desprez, M., 2000. Physical and biological impact of marine aggregate extraction along the French coast of the eastern English Channel: short and long-term post-dredging restoration. *ICES Journal of Marine Science,* 57(5), 1428–1438.
Desprez, M.; Pearce, B., and Le Bot, S., 2010. The biological impact of overflowing sands around a marine aggregate extraction site: Dieppe (eastern English Channel). *ICES Journal of Marine Science,* 67, 270–277.
Dickson, R.R. and Rees J.M., 1998. *Impact of Dredging Plumes on Race Bank and Surrounding Areas*. CEFAS, LOWESTOFT. Unpublished Final Report to MAFF, U.K., 15p.
Dupont, J.; Lafite, R., and Lamboy, M., 1985. *Contribution de l'étude des Suspensions à la Comprehension des Mecanismes Hydro-sedimentaires Estuariens et Littoraux en Manche Centrale et Orientale*. La Baie de Seine (GRECO-MANCHE)—Colloque National du CNRS. Plouzané, France: Ifremer, pp. 145–153.
Folk, R.L., 1954. The distinction between grain-size and mineral composition in sedimentary rock nomenclature. *Journal of Geology,* 62(4), 344–359.
Francois, R.E. and Garrison, G.R., 1982a. Sound absorption based on ocean measurements, part I: pure water and magnesium sulfate contributions. *Journal of the Acoustical Society of America,* 72(3), 896–907.
Francois, R.E. and Garrison, G.R., 1982b. Sound absorption based on ocean measurements, part II: boric acid contribution and equation for total absorption. *Journal of the Acoustical Society of America,* 72(6), 1879–1890.
Gajewski, L.S. and Uscinowicz, S., 1993. Hydrologic and sedimentologic aspects of mining marine aggregate from the Slupsk Bank (Baltic Sea). *Marine Georesources and Geotechnology,* 11(3), 229–244.
Gartner, J.W., 2004. Estimating suspended solids concentrations from backscatter intensity measured by acoustic Doppler current profiler in San Francisco Bay, California, *Marine Geology,* 211(3), 169–187.
Gentil, F., 1976. Distribution des Peuplements Benthiques en Baie de Seine. Paris: University of Paris 6, Ph.D thesis, 470p.
Hitchcock, D.R. and Bell, S., 2004. Physical impacts of marine aggregate dredging on seabed resources in coastal deposits. *Journal of Coastal Research,* 20(1), 101–114.
Hitchcock, D.R. and Drucker, B.S., 1996. Investigation of benthic and surface plumes associated with marine aggregate mining in the United Kingdom. *In: The Global Ocean—Towards Operational Oceanography: Proceedings of the Oceanology International 1996 Conference* (Oceanology International, Spearhead, Surrey), pp. 221–234.
Hitchcock, D.R.; Newell, R.C., and Seiderer, L.J., 1999. *Investigation of Benthic and Surface Plumes Associated with Marine Aggregate Mining in the United Kingdom—Final Report* (Contract Report for the U.S. Department of the Interior, Minerals Management Service, Contract No. 14-35-0001-30763). Cornwall, UK: Coastline Surveys, Ref. 98-555-03.
Hitchcock, D.R.; Newell, R.C., and Seiderer, L.J., 2002. *Integrated Report on the Impact of Marine Aggregate Dredging on Physical and Biological Resources of the Sea Bed*. Washington, DC: U.S. Department of the Interior, Minerals Management Service, International Activities and Marine Minerals Division (INTERMAR), OCS Report No. 2000-054.
HR Wallingford, 2011. *Area 473 East. Dredger and Plume Monitoring Study*. Howbery Park, UK: HR Wallingford, Report EX 6215, Release 3.0, February 2011, 390p.
ICES (International Council for the Exploration of the Sea), 2009. *Effects of Extraction of Marine Sediments on the Marine Ecosystem*. Copenhagen, Denmark: ICES Cooperative Research Report 297, 182p.
Larsonneur, C., 1971. Manche Centrale et Baie de Seine: Géologie du Substratum et des Dépôts Meubles. Caen, France: University of Caen, Ph.D thesis, 394p.
Lafite, R.; Dupont, J.P., and Lamboy, M., 1985. *Stratégie d'étude des Suspensions Mise en Oeuvre en Baie de Seine*. La Baie de Seine (Greco Manche)—Colloque National du CNRS. Plouzané, France: Ifremer, pp. 135–144.
Le Bot S.; Lafite, R.; Fournier, M.; Baltzer, A., and Desprez, M., 2010. Morphological and sedimentary impacts and recovery on a mixed sandy to pebbly seabed exposed to marine aggregate extraction (Eastern English Channel, France). *Estuarine, Coastal and Shelf Science,* 89(3), 221–233.
Mikkelsen, O.A. and Pejrup, M., 2000. *In situ* particle size spectra and density of particle aggregates in a dredging plume. *Marine Geology,* 70(16), 443–459.
Newell, R.C.; Seiderer, L.J.; Simpson, N.M., and Robinson, J.E., 2002. *Impact of Marine Aggregate Dredging and Overboard Screening on Benthic Biological Resources in the Central North Sea: Production Licence Area 408, Coal Pit*. Bath, UK: Marine Ecological Surveys, Ltd., Technical Report.
Newell, R.C.; Seiderer, L.J.; Simpson, L.J., and Robinson, J.E., 2004. Impacts of marine aggregate dredging on benthic macrofauna off the south coast of the United Kingdom. *Journal of Marine Research,* 20(1), 115–125.
Robinson, J.E.; Newell, R.C.; Seiderer, L.J., and Simpson, N.M., 2005. Impacts of aggregate dredging on sediment composition and associated benthic fauna at an offshore dredge site in the southern North Sea. *Marine Environmental Research,* 60(1), 51–68.
SHOM (Service Hydrographique et Océanographique de la Marine), 2009. Annuaire des Marées—Tome 1. Brest, France: SHOM, 208p.
Smith, S.J. and Friedrichs, C.T., 2011. Size and settling velocities of cohesive flocs and suspended sediment aggregates in a trailing suction hopper dredge plume. *Continental Shelf Research,* 31(10), S50–S63.
Spearman, J.; Bray, R.N.; Land, J.; Burt, T.N.; Mead, C.T., and Scott, D., 2007. Plume dispersion modeling using dynamic representation of trailer dredger source terms. *In:* Maa J.P.-Y.; Sanford L.P., and Schoellhamer D.H. (eds.), *Estuarine and Coastal Fine Sediment Dynamics*. Amsterdam: Elsevier, pp. 417–448.
Stelzenmüller, V.; Ellis, J.R., and Rogers S.I., 2010. Towards a spatially explicit risk assessment for marine management: assessing the vulnerability of fish to aggregate extraction. *Biological Conservation,* 143(1), 230–238.
Tessier, C.; Le Hir, P.; Lurton, X., and Castaing, P., 2008. Estimation de la matière en suspension à partir de l'intensité rétrodiffusée des courantomètres acoustiques à effet Doppler (ADCP). *Comptes Rendus Geosciences,* 340(1), 57–67.
TRDI (Teledyne RD Instruments), 2007. *WinRiver II User's Guide*. Pittsburgh, PA: TRDI, P/N 957-6231-00, 48p.
Truitt, C.L., 1988. Dredged material behaviour during open water disposal. *Journal of Coastal Research,* 4(3), 389–397.
Whiteside, P.G.D.; Ooms, K., and Postma, G.M., 1995. Generation and decay of sediment plumes from sand dredging overflow. *In: Proceedings of the 14th World Dredging Congress*. Delft, The Netherlands: World Organisation of Dredging Associations, pp. 877–892.
Winterwerp, J.C., 2002. Near-field behaviour of dredging spill in shallow water. *Journal of Waterway, Port, Coastal and Ocean Engineering,* 128(2), 96–98.
Zanke, U., 1977. *Berechnung der Sinkgeschwindigkeiten von Sedimenten*. Hannover, Deutschland: Mitt. Des Franzius-Institut für Wasserbau, Heft 46, Seite 243, Technical University.